

## PUPIL DENSIFICATION: A PANORAMA

Frantz Martinache<sup>1</sup> and Olivier Lardière<sup>2</sup>

**Abstract.** The technique of pupil densification bridges the gap existing between conventional optical astronomy observing techniques and optical interferometry: it indeed leads to the concept of hypertelescope: an instrument that can provide direct images at the focus of an interferometer. The hypertelescope is the open sesame for high dynamic imaging with an interferometer: indeed, the elementary remapping of the pupil operated by a densifier not only maximizes the dynamic range and the signal to noise ratio of images but also makes the interferometer compatible with most existing coronagraphic devices. Moreover, a careful discussion about field of view show that for a diluted array, the pupil densification preserves all the relevant high angular resolution information collected by the interferometer and therefore induces no field loss.

### 1 Introduction

The development of optical interferometry techniques has been a breakthrough that brutally gave birth to instruments with extreme resolving power. Yet, if optical interferometry it has proven to be an powerful tool for astronomy, it still has to demonstrate wide field imaging capabilities. The reason for the absence of such images is that, unlike their radio equivalent (*e.g.* VLA (1976)), current optical interferometers do not use more than 3-4 telescopes at a time: Optical interferometry produces extremely precise measurements, but there are not enough of these measurements to provide images of arbitrarily complex sources. The recent progress in wavefront control, such as adaptive optics, however now make ambitious kilometric scale projects involving telescopes by the dozen possible, in both ground-based or spaceborne versions.

This paper focuses on a family of interferometers for which the pupil is diluted, *i.e.* for which the diameter of each sub-aperture can be considered point-like,

---

<sup>1</sup> Cornell University, USA

<sup>2</sup> Observatoire de Haute Provence, France

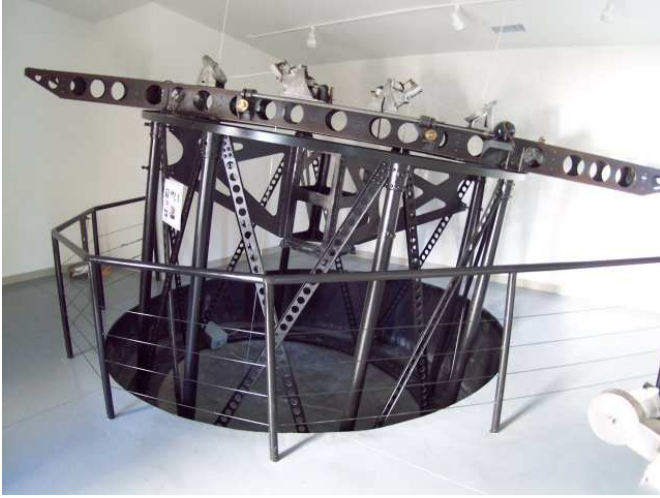


**Fig. 1.** Michelson's historical interferometer now resting in the CHARA mini-museum at Mt Wilson Observatory. It was originally installed on the top of the 100" Hooke Telescope and provided the first stellar diameter measurement (1921).

compared to the baseline of the interferometer itself. For well-populated, sparse array of telescopes, direct imaging has been proved feasible with the technique of pupil densification proposed by Labeyrie (1996). Pupil densification however already started with Michelson's stellar interferometer experiment and is still going on in the many existing OI projects, because of its convenience.

Because he needed to combine two 20 feet separated beams in the 100" Hooke telescope, Michelson used a periscopic arrangement of flat mirrors (see fig. 1) so that, seen from the detector, the two beams appear closer than seen from the sky. This remapping of the pupil, deployed because of hardware limitations, accidentally intensified the fringes and facilitated the measurement of visibilities when no electronic detectors were available !

The idea of using an interferometer for optical high angular direct imaging was raised in the 80's. Traub (1986) publishes a paper in which he states a "golden rule of imaging interferometers" according to which, only a combiner that provides an exit pupil homothetic to the entrance one can produce direct images with a invariant translation point spread function (PSF). This therefore excluded Michelson-like interferometers and makes the purely homothetic (classically called Fizeau) observing mode the only option. The golden rule however proved to be too restrictive: on the one hand, Tallon & Tallon-Bosc (1992) showed that for monochromatic observations, the information *a priori* lost with the Michelson beam combiner can be restored by a post-detection treatment of the data. On the other hand, Labeyrie (1996) demonstrated that direct imaging is still possible with a Michelson-like interferometer and proposed a modified golden rule: one has respects the geometry of the centers of sub-apertures only. Labeyrie's  $n$ -aperture

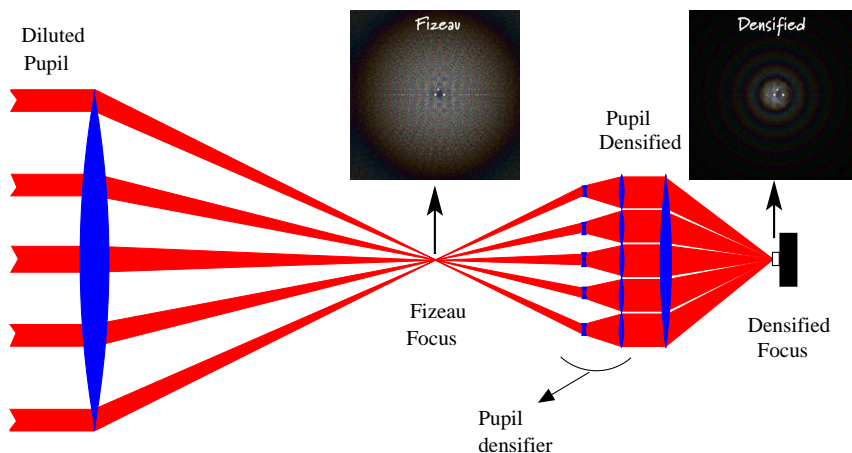


**Fig. 2.** Michelson’s non homothetic combining mode generalized to a  $n$ -aperture interferometer. The densifier, made of inverted Galilean telescopes makes the sub apertures edge-to-edge in the output pupil: this results in a much better contrasted PSF, allows direct imaging and eventually the use of coronagraphic techniques.

generalization of the Michelson interferometer exhibit remarkable features adapted for direct imaging and coronagraphy but seems to come at the expense of a reduction of the field of view (hereafter abbreviated FOV).

## 2 The Hypertelescope concept

In the Fizeau combining mode, the PSF of a diluted aperture is made of a central white peak surrounded by a extended dispersed halo of sidelobes that, depending on the geometry of the array, can either be well ordered peaks or pseudo-random speckles and spread over a wide area. Low dynamic range and wide size make it poorly suited for direct high angular resolution imaging and totally incompatible for most coronagraphic devices.

Labeyrie proposes to compensate this weakness of the Fizeau image with a generalization Michelson’s design: a “densified-pupil multi-aperture imaging interferometer” also called “hypertelescope”. The figure 2 sketches how Labeyrie suggests to densify the pupil, by using, after the Fizeau focal plane, a densifier, that zooms each sub-aperture but preserves the geometry of the array. The densification is characterized by a coefficient  $\gamma$  defined by the following ratio:

$$\gamma = \frac{d_o/D_o}{d_i/D_i}, \quad (2.1)$$

where  $D$  and  $d$  respectively represent the diameter of the interferometer and one sub-aperture, indices  $i$  and  $o$  respectively designing the input and output pupil.

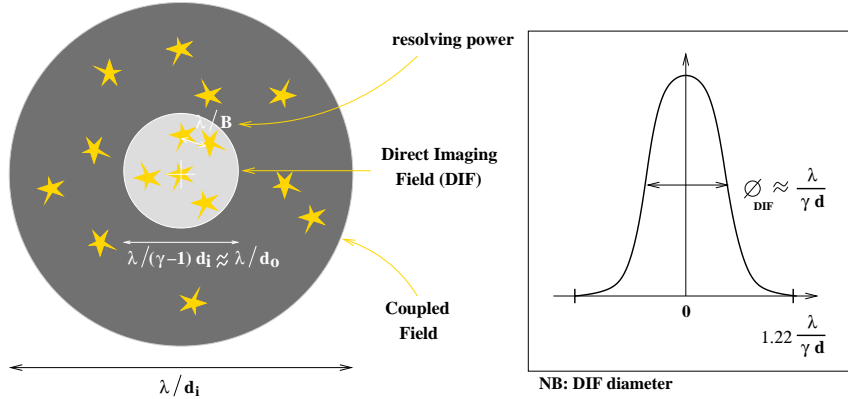


**Fig. 3.** Characteristic dimensions of the hypertelescope FOV. The coupled field is imposed by the diameter of a sub-aperture in the input pupil  $\lambda/d_i$ . The Direct Imaging Field (DIF) is imposed by the diameter of a sub-aperture in the output pupil  $\lambda/d_o$ . High Angular Resolution information is preserved and the resolving power remains  $\lambda/D$ .

$\gamma = 1$  corresponds to the Fizeau combining scheme for which the input and output pupil are homothetic.

On axis, the effect of a densification ( $\gamma > 1$ ) is extremely positive, since it doesn't alter the phase: the halo of sidelobes simply shrinks and because the energy collected by the interferometer, the central peak is intensified by a factor  $\gamma^2$ . Off-axis however, the remapping decreases the slope of the wavefront inside each sub-aperture, with respect to the average wavefront slope. When the sub-apertures are point-like compared to the diameter of the interferometer, the densification can be so strong ( $\gamma \gg 1$ ) that the halo doesn't even move anymore, while the white peak moves like in the Fizeau case (see the comparison of Fizeau and densified images of a triple star on fig. 2).

The PSF therefore becomes non translation-invariant: when the peak reaches the edge of the halo<sup>1</sup>, it becomes undetectable. With pupil densification, direct imaging is possible in a FOV reduced to the halo of a densified sub-aperture. The diameter of this Direct Imaging Field (DIF) is therefore:

$$DIF = \frac{\lambda}{\gamma d}. \quad (2.2)$$

Inside this DIF, Labeyrie 1996 demonstrates that the image of an extended source can be written as a pseudo-convolution relation:

$$I(x, y) = \frac{A(x, y)}{\gamma_D^2} \times \left( O\left(\frac{x}{\gamma_D}, \frac{y}{\gamma_D}\right) \otimes Int(x, y) \right), \quad (2.3)$$

<sup>1</sup>fig. 3 shows that the border of the DIF is actually somewhat halfway to the edge of the halo

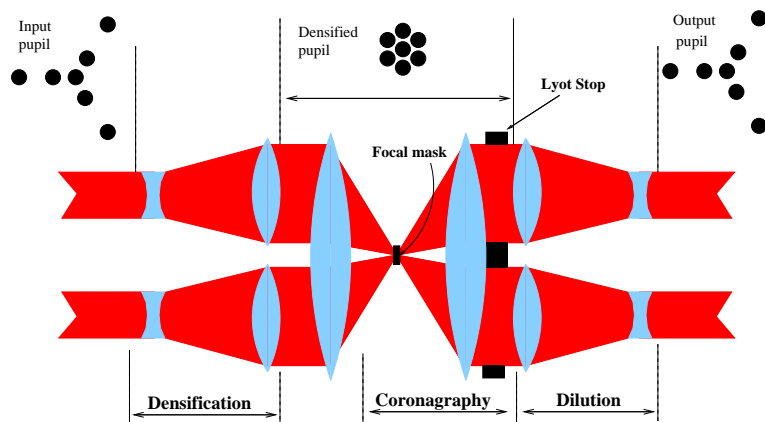


**Fig. 4.** Process of Densification-Dilution: the pupil is first densified to make it more compatible with the coronagraph and then diluted with an inverted copy of the densifier to restore the field.

where  $A(x, y)$  represents the diffraction lobe of a densified sub-aperture and  $Int(x, y)$  the interference function, *i.e.* the PSF of an interferometer made of dot-like sub-apertures, whose positions For a diluted aperture, the densification is so strong (*i.e.*  $\gamma_D \gg 1$ ) that one may consider the envelope position fixed for all sources located inside the useful FOV.

### 3 Anarchic pupil remapping

According to Guyon & Roddier (2002), the advantage offered by pupil densification is the possibility to use coronagraphy at the focus of the interferometer. As a consequence, after the coronagraph, these authors suggest recovery of wide field imaging capabilities of the Fizeau by using an exact copy of the densifier, working backwards and therefore re-diluting the pupil before the detector (*c.f.* fig. 4). Because of this final remapping, Labeyrie’s modified version of the golden rule doesn’t need to apply anymore: one can remap the pupil in a complete “anarchic” way as long as the pupil is restored before the final detector.

The use of this second remapping can be seen as an optical equivalent of the Tallon & Tallon-Bosc (1992) post-detection correction technique mentioned earlier. The big advantage this pre-detection correction is its natural achromaticity. One shall mention that this idea of double pupil remapping for coronagraphic devices lead Guyon (2003) to a peculiarly efficient coronagraphic device: the PIAAC (see also Martinache (2006) in these proceedings).

Yet, the use of an anarchic remapping for coronagraphy at the focus of an interferometer is questionable: because it doesn’t respect the modified version of the golden rule, the FOV in the intermediate focal plane becomes rigorously null. Even if this is corrected by the dilution of the pupil after the occulting mask

(see fig. 4), the coronagraph becomes extremely sensitive to both pointing errors and partial resolution of the observed source, that are absolutely non-negligible for an interferometer. Increasing the size of the occulting mask does not compensate this leak since the light of any barely off-axis source spreads over the whole FOV. Labeyrie’s homothetic remapping provides a pseudo-convolution relation: it can therefore naturally deal with partially resolved objects. Moreover, we shall see the fundamental limit for the imaging of a wide FOV is not imposed by the hypertelescope combining mode, but by the geometry of the array itself.

## 4 FOV considerations

In our attempt to make an interferometer look like a “friendlier” giant telescope, one has to keep in mind an essential specificity of diluted interferometers: they only provide a discrete coverage of the spatial frequency plane. For this reason only, an interferometer, using pupil densification or not, cannot provide images of arbitrarily complex sources and/or arbitrarily wide field. This discussion requires the introduction of three different FOV, whose properties will be detailed in the following subsections:

- The “Interferometric Field” (IF) whose maximum extent is imposed by the number of independent baselines offered by the geometry of the array.
- The “Direct Imaging Field” (DIF) is simply the field over which direct imaging of a source is possible. This field is of course only function of the beam combination scheme.
- The “Coupled Field” (CF) is the field defined by the fraction of the sky that will see at least a part of its light on the central pixel of the detector, for better or for worse. This field also depends on the retained beam combiner.

### 4.1 Interferometric Field (IF)

Simply relying on the Nyquist-Shannon sampling theorem, a well-known rule coming from radio-astronomy reminds that: “The mappable field of view of an interferometer is given by the largest typical hole in the (u,v) coverage”, i.e the minimum distance between telescopes. An illustration of the clean part of the PSF (direct or pairwise-synthesized) is given at the figure 5.

An upper limit of the IF can be found using the information theory of Shannon (1948). Without ever considering a combination scheme, Koechlin (2003) demonstrates that for an interferometer, the ratio field/resolution is only constrained by the number of telescopes involved in one observation and by the dynamic range of measurements. One can invoke on the one hand, Shannon’s entropy collected in an observation:

$$H \leq n_{obs} \log_2(\delta_{data}), \quad (4.1)$$

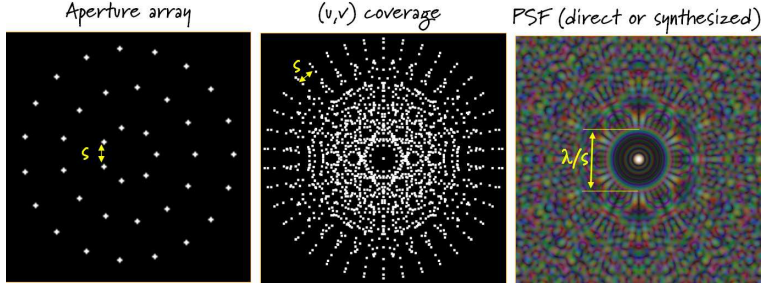


**Fig. 5.** The clean field of an interferometric PSF is given by  $\lambda/s$  where  $s$  is the minimal distance between the telescopes.  $s$  is also the typical largest gap of the  $(u,v)$  coverage.

where  $n_{obs}$  is the number of observables and  $\delta_{data}$  the dynamic range of measurements. A non-redundant cophased interferometer involving  $n_T$  telescopes gives  $n_B = n_T \times (n_T - 1)/2$  complex visibilities, that is  $n_{obs} = 2 \times n_B$  (modulus and phase).

On the other hand, the entropy of the image reconstructed from these interferometric data is given by:

$$H_{ima} = n_r \log_2(\delta_r), \quad (4.2)$$

where  $n_r$  and  $\delta_r$  are respectively the number and the dynamic-range of pixels in the image.

In the most favorable case, these two entropy terms can be made equal. This therefore constrains the number of resels in one image as  $n_r \leq n_T \times (n_T - 1)$ . Since the angular size of one resel is  $\lambda/B$  (with  $B$  the maximum baseline), the extent of this interferometric field is given by:

$$IF \leq \lambda/B \times \sqrt{n_T \times (n_T - 1)}. \quad (4.3)$$

This is a very strong field limitation that is absolutely independent on the beam combination scheme.

#### 4.2 Direct imaging field (DIF)

The DIF however, depends only on the beam combination scheme. As already mentionned, for a hypertelescope, the diameter of the DIF is given by:

$$DIF = \frac{\lambda}{(\gamma - 1) d} \quad (4.4)$$

where  $\gamma$  is the pupil densification factor and  $d$  the diameter of a single telescope. It is this apparent reduction of the DIF (infinite in the Fizeau case for which  $\gamma = 1$ ) by the factor  $\gamma - 1$  that leads to the conclusion that the hypertelescope induces field loss.

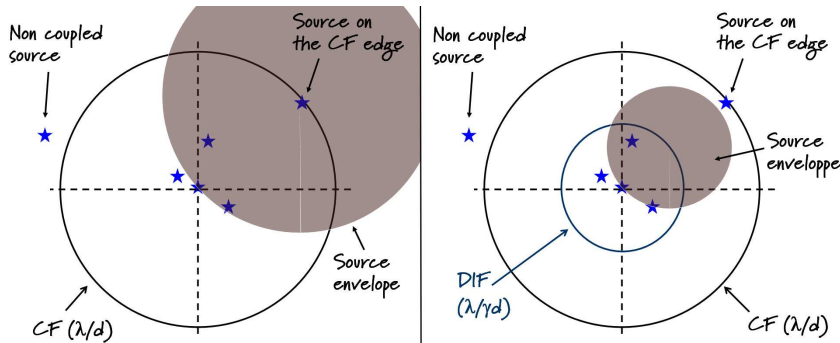


**Fig. 6.** Comparison of coupled fields for both Fizeau (left) and hypertelescope (right) observing modes: the limit is the same.

The densification coefficient is however a free parameter that we can use to merge the DIF and the IF as proposed in Martinache (2005). The equality of those two fields leads to the value of an optimal densification coefficient:

$$\gamma_{opt} = 1 + \frac{B}{d\sqrt{n_T \times (n_T - 1)}} \approx \frac{B}{d \times n_T}. \quad (4.5)$$

This coefficient can definitely be said optimal since it concentrates the flux as much as possible, without destroying any information: it preserves the entropy.

For an “in-line” redundant interferometer, this optimal densification is achieved when sub-apertures are made edge to edge in the output pupil, exactly as Labeyrie initially proposed, without any consideration for the field of view. This result can indeed be intuited when one realizes that when the densification that merges the DIF to the clean part of the interferometric PSF (c.f. fig. 5) is for  $\gamma = s/d$ , meaning that the sub-pupils in the output pupil have to be edge to edge: the hypertelescope induces no field loss.

### 4.3 Coupled field (CF) and crowding limit

One can define the coupled field this way: if a source belongs to the CF, its light will appear on the final detector. The notion of CF is essential in interferometry, for the extent of the CF decides whether or not the interferometer can obtain an image of an object from a given area of the sky.

Defining the IF, we’ve indeed seen that the sparse coverage of the u-v plane by the interferometer only provides limited information. This also imposes the maximum acceptable complexity of a target field, which is known as the *crowding limit* of the interferometer.

Each source produces a central peak resulting from  $n_T$  coherent contributions and a halo resulting from the same number of incoherent contributions: the peak intensity scales as  $n_T^2$ , while the average level of the halo scales as  $n_T$ . Peaks are

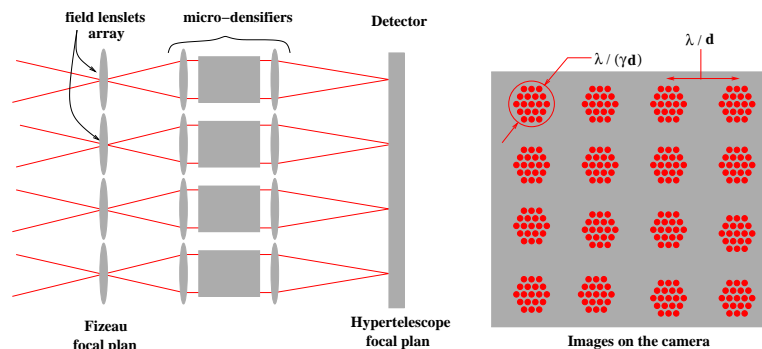


**Fig. 7.** Multi-field observing mode is naturally possible thanks to the passage by the Fizeau focus. Labeyrie (2004) proposes to multiplex the densifier and therefore provide simultaneous direct images, covering a FOV much wider than the DIF.

detectable if they dominate the fluctuations of the halo, which is  $\sqrt{p} n_T$  with  $p$  the number of coupled sources. Then we have to meet the condition  $n_T \geq \sqrt{p} n_T$ , meaning that  $p \leq n_T^2$ : the number of coupled sources must be kept lower than the number of baselines. If the complexity of a source is greater than this crowding limit, one needs *a priori* knowledge on the source to be able reconstruct an image.

The figure 6 shows that there is no difference between Fizeau and hypertelescope:  $CF = \lambda/d_i$ . A difference however appears when the interferences are recorded in a pupil plane as proposed by Vakili *et al.* (2004): the CF becomes infinite and the crowding becomes a serious issue. The use of a spatial filtering (pinhole or single mode fiber) to evade this limit makes both image-plane and pupil-plane interferometers equivalent again.

## 5 Beyond the coupled field

Yet, even if the DIF is limited, high angular resolution astrometric measurements are possible over a theoretically infinite FOV. The Fizeau focus (for which the DIF is large) offers a natural opportunity to do what is usually called dual or multiple field observing mode, for sources at least separated by  $\lambda/d$ , using neither beam splitter nor supplementary delay lines. Labeyrie (2004) takes advantage of this ideal configuration: one can use two or more independant densifiers that can image fractions of the sky at least separated by  $\lambda/d_i$ : direct imaging is now possible over a large FOV. Figure 7 sketches one possible design for multi-field direct imaging.

## 6 What about already dense apertures ?

The introduction suggested that pupil densification for direct imaging should be applied to diluted apertures only. Aime *et al.* (2003) attempt to extrapolate the

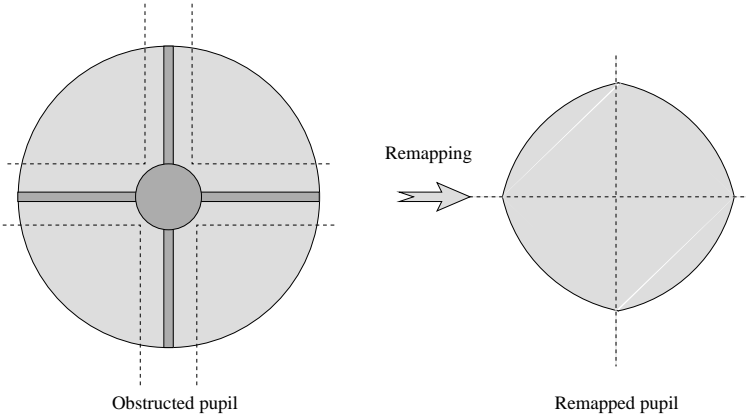


**Fig. 8.** Pupil remapping of an obstructed monolithic aperture: get rid of the pupil obscuration for high performance coronagraphy. Adapted from Aime *et al.* (2003).

use of pupil densification to obstructed monolithic apertures. Their motivation is to get rid of the obstruction of the pupil by the secondary mirror and the “spider” structure bearing it. Indeed, the presence of such an obscuration severely compromises the performance of most high contrast coronagraphic device. For a non-resolved source in ideal observing conditions, a remapping such as the one presented on fig. 8 will produce the expected effect.

These authors however notice that such a remapping only offers a very small DIF. This is not surprising since the situation is very similar to Guyon’s anarchic remapping presented in sect. 3. The conclusions and remarks already mentioned then shall therefore apply again: to recover wide field imaging capabilities, one needs to restore the geometry of the pupil after the coronagraphic mask.

For the coronagraphy of a perfectly non-resolved on-axis source, this technique may prove useful. However, the relevance of these ideal hypothesis is quite questionable: at high level of contrast (*i.e.* over  $10^4$ ), partial resolution of the source and residual tip-tilt induce leaks that seriously compromise the performance of coronagraphy, for both interferometers and monolithic telescopes. This issue of high contrast coronagraphy will very probably find its solution with the development of efficient aposization techniques.

## 7 Conclusion

To make direct imaging with an optical interferometer a reality, many technical issues still have to be solved. The main challenge remains the control of the wavefront. Better Adaptive Optics and cophasing systems will increase the sensibility of observations and make the hypertelescope observing mode possible at the focus of any interferometer, on the ground or in space.

Using field of view considerations, we’ve seen that an hypertelescope can be

seen as an optical technique of image reconstruction that optimizes the signal to noise and preserves all relevant high angular resolution information collected by the interferometer. In the presence of sky background and with a noisy (dark current and readout noise) detector, it makes possible the imaging of objects too faint for the Fizeau and pairwise fringe acquisition observing modes. In terms of field of view, its limitations are due to the geometry of the array only.

One should finally mention the existence of two distinct project that share the ambition of direct imaging with an interferometer: VIDA, by Lardière *et al.* (2006), is a precursor hypertelescope that would use the already existing infrastructure of VLTI and Carina, by Le Coroller *et al.* (2004), a project of interferometer made for the hypertelescope observing mode, involving dozens of small mirrors, at the present time in construction at Observatoire de Haute Provence.

## References

- Aime, C. *et al.* 2003, EAS Publ. Series, 8, 281.  
 Michelson, A. & Pease, F. 1921, ApJ, 53, 249.  
 Labeyrie, A. 1996, A&AS, 118, 517.  
 Labeyrie, A. 2004, Lecture at College de France.  
 Le Coroller, H. 2005, A&A, 426, 721.  
 Guyon, O. & Roddier, F. 2002, A&A, 391, 379.  
 Guyon, O. 2003, A&A, 404, 379.  
 Koechlin, L. 2003, EAS Publ. Series, 8, 349.  
 Lardiere, O. *et al.* 2006, in prep.  
 Lardiere, O. *et al.* 2005, JENAM conf. proc.  
 Martinache, F. & Lardiere, O. 2005, JENAM conf. proc.  
 Martinache, F. 2005, PhD Dissertation.  
 Martinache, F. 2006, these proceedings.  
 Shannon, C. E. 1948, BSTJ, 27, 379.  
 Tallon, M. & Tallon-Bosc, I. 1992, A&A, 253, 641.  
 Traub, W. 1986, Appl. Opt, 25, 528.  
 Vakili, F. *et al.* 2004, A&A, 421, 147.  
 The VLA takes place 1976, S&T, 52, 320.